Int. J. Electrochem. Sci., 8 **(2013)** 10890 - 10902

International Journal of
ELECTROCHEMICAL
SCIENCE
www.electrochemsci.org

Microwave Assisted Green Synthesis of Bis-Phenol Polymer Containing Piperazine as a Corrosion Inhibitor for Mild Steel in 1M HCl

Priyanka Singh[1], *M.A. Quraishi*[1,*], *Eno E. Ebenso*[2]

[1]Department of Applied Chemistry, Indian Institute of Technology, Banaras Hindu University, Varanasi-221005
2 Material Science Innovation & Modelling (MaSIM) Research Focus Area, Faculty of Agriculture, Science and Technology, North-West University (Mafikeng Campus), Private Bag X2046, Mmabatho 2735, South Africa
[*]E-mail: maquraishi@rediffmail.com; maquraishi.apc@itbhu.ac.in

Received: 25 May 2013 / *Accepted:* 11 July 2013 / *Published:* 1 August 2013

Microwave-assisted organic synthesis involves simple work procedure and gives high yield of product. In view of this we have synthesized bis-phenol formaldehyde polymer containing piperazine by microwave technique and investigated its inhibition action on corrosion of mild steel in 1 M HCl using gravimetric, electrochemical impedance spectroscopy (EIS), linear polarization resistance (LPR) and potentiodynamic polarization techniques. The Tafel polarization study reveals that inhibitor acts as mixed-type inhibitor. EIS study indicates that it inhibits corrosion by adsorption mechanism. The adsorption of polymer on mild steel followed Langmuir adsorption isotherm. In optical microscopy examination inhibited mild steel surface was found to be smoother than uninhibited mild steel surface.

Keywords: BFP Polymer (condense polymer of Bisphenol, Formaldehyde and Piperazine), Mild steel (MS), Gravimetric Measurements, Electrochemical measurements and Optical microscopy.

1. INTRODUCTION

The use of Microwave irradiation for synthesis of organic compounds is one of the important techniques in green chemistry. The benefits of microwave technique are as follows: it accelerates rate of reaction which reduces time from days and hours to minutes, reduce side reactions, increase yields, improves reproducibility and make synthesis method easier than conventional heating [1].Organic Polymer constitute a potential class of corrosion inhibitors .The corrosion inhibition performance of these compounds is attributed due to the presence of Π electrons, heteroatoms and large molecular size

which ensures greater coverage of metal by the molecules and leads to more inhibition efficiency [2-8].

In the present investigation we have synthesized bis-phenol polymer containing piperazine by microwave technique to study its inhibition property on corrosion of mild steel in 1 M HCl by using weight loss, electrochemical impedance spectroscopy (EIS), linear polarization resistance (LPR) and potentiodynamic polarization techniques.

2. EXPERIMENTAL

2.1. Materials and Solutions

The MS having following composition (wt. %): 0 .076% C, 0.192% Mn, 0.012% P, 0.026% Si, 0.050% Cr, 0.023% Al, 0.123% Cu and remaining Fe were used to perform experiment. For weight loss studies the dimensions of MS coupons can be 2.5 cm × 2 cm × 0.025 cm. The MS strip which was used as working electrode in electrochemical study having such dimensions of 8 cm × 1 cm × 0.025 cm sizes with an exposed area of 1 cm^2 and rest being covered by epoxy resin. The analytical grade of 37% HCl diluted with double-distilled water used to prepare 1M HCl test solution. The stock solution of BFP polymer which was used as inhibitor was prepared in 1 M HCl containing 1% acetone.

2.2. Synthesis of BFP polymer

The (BFP) polymeric compound was synthesized the by condensation of bisphenol-A, formaldehyde, and piperazine in alkaline medium (Scheme 1). In a 100mL three-necked round-bottom flask, 2.28 g of bisphenol-A and 1.5mL of formaldehyde (37% aqueous solution) were combined and the pH was adjusted to 8 with sodium hydroxide. The mixture was then kept in microwave with continuous stirring at 70 °C for first step and then 0.86 g of piperazine was added in the reaction mixture and stirred again at 70°C. The experimental conditions are shown in Table 1. The reaction was monitored by thin layer chromatography (TLC) using ethanol as eluent. The reaction mixture was cooled, precipitated into deionised water, and filtered. A white powder solid product was obtained with good yield [9].

Table 1. Optimization of reaction conditions for BFP polymer

Condition (W)	Temperature (°C)	Step I *t* (min)	Step II *t* (min)	Yield (%)
300	70	15	5	39
400	70	15	5	53
500	70	15	5	71
700	70	15	5	76

2.3 Characterization of BFP polymer

IR frequencies of BFP polymer show a band at 3346 cm^{-1} due to phenolic OH. The presence of methylene was confirmed by strong bands at 2818 cm^{-1} due to ν C–H asymmetric and symmetric stretching. In BFP polymer a sharp band at 1498–1464 cm^{-1} due to δCH2 bending and peaks between 1612 and 1595 cm^{-1} are attributed to aromatic C=C stretching. All the compounds show absorptions between 1255 and 1003 cm^{-1} due to aliphatic C–N and the polymeric compounds show characteristic bands at 2964 cm^{-1} due to aromatic ν C–H. In BFP polymer a sharp peak at 1.59 and 1.61 ppm was assigned due to –CH3 protons. The protons of Ar–CH2–N and N–CH2–CH2–N appeared at 2.9 and 2.4 ppm. The OH attached to CH2 appeared at 3.6 and of aromatic protons appeared between 6.6 and 6.7 and multiplets at 7.0-7.2 ppm was assigned to Ar–OH.

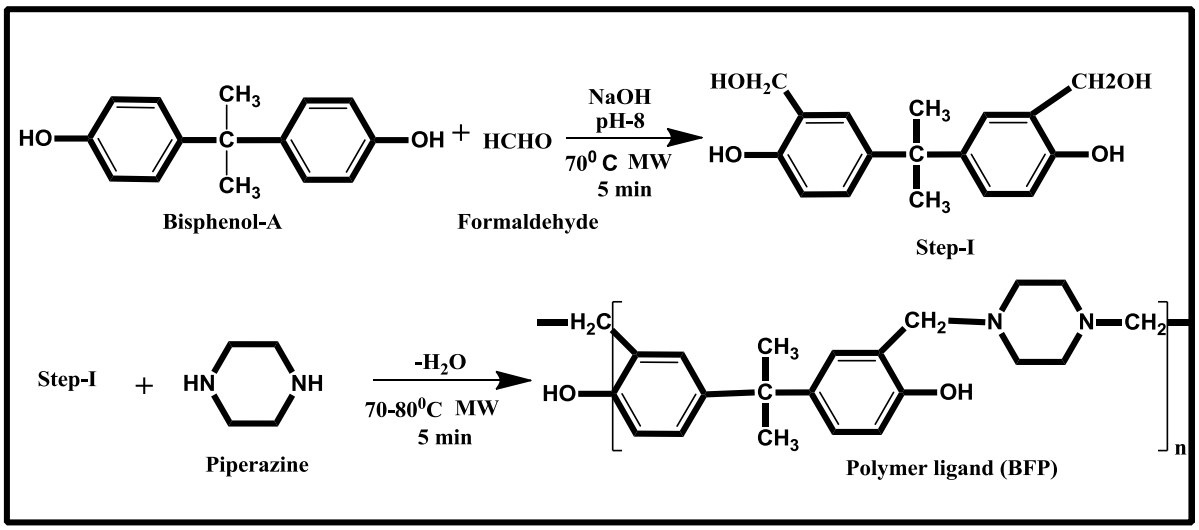

Scheme 1. Synthesis of BFP polymer

2.4. Gravimetric measurements

MS specimens having area (2.5 cm ×2.0 cm ×0.025 cm) were abraded with different grades of emery paper (600-1200 grades) and washed with distilled water and finally with acetone. The weighed specimens were immersed in 100 ml of 1M HCl acid solution with and without inhibitor for 3h at 35 ° C. After 3 h specimen were taken out, washed, dried and weighed accurately. All the tests were repeated at different temperatures. The corrosion rate (C_R) was calculated from the following equation,

$$C_R\,(\mathrm{mm/y}) = \frac{87.6W}{atD} \qquad (1)$$

where W is the average weight loss of MS specimens, a total area of one MS specimen, t is the immersion time (3 h) and D is density of MS in (gcm^{-3}). The inhibition efficiency (η %) of inhibitor for the corrosion of MS was calculated as follows,

$$\eta\% = \frac{C_R - {}^{inh}C_R}{C_R}\ \mathrm{X}\ 100 \qquad (2)$$

where C_R and ${}^{inh}C_R$ are the corrosion rates of MS in the absence and presence of the inhibitors, respectively.

2.5. Electrochemical measurements

Electrochemical studies were carried out in the three electrode cell assembly connected to Potentiostat/Galvanostat G300-45050 (Gamry Instruments Inc., USA) Echem Analyst 5.0 software package. Mild steel was used as working electrode with an exposed area of 1 cm^2, platinum electrode as an auxiliary electrode, and saturated calomel electrode (SCE) as reference electrode. All potentials were measured versus a saturated calomel electrode (SCE) i.e. reference electrode. Tafel curves were obtained by changing the electrode potential automatically from −0.25 V to +0.25 V versus open corrosion potential at a scan rate of 1.0 mVs^{-1}. Linear Polarization Resistance (LPR) experiments were done from −0.02 V to +0.02 V versus open corrosion potential at the scan rate of 0.125mVs^{-1}. EIS measurements were performed under potentiostatic conditions in a frequency range from 100 kHz to 0.01 Hz, with amplitude of 10mV AC signal. All experiments were measured after immersion period for 30 min of MS in 1 M HCl in absence and presence of different concentration of inhibitor.

3. RESULTS AND DISCUSSION

3.1. Electrochemical measurements

3.1.1. Potentiodynamic polarization and linear polarization resistance

Table 2. Polarization data for MS in 1 M HCl in absence and presence of different concentration of BFP polymer

	Tafel Polarization					Linear Polarization	
Inhibitor concentration (ppm)	E_{corr} (mV vs SCE)	β_a (mV/dec)	β_c (mV/dec)	I_{corr} (μA cm^2)	η%	R_p (Ω cm^2)	η%
Blank	-448	46	96	1070	-	14.0	-
5	-488	79	148	389	63.6	64.8	78.3
15	-491	92	236	271	74.6	89.4	84.3
50	-499	69	95	74	93.0	203.9	93.1
75	-520	101	161	64	94.0	302.4	95.3

The polarization curves for mild steel in 1 M HCl in presence and absence of polymer is shown in Figure 2. The various electrochemical parameters calculated for tafel plot are given in Table 2. It is seen that addition of polymer decreases I_{corr} values. At 75 ppm optimum concentration of polymer

reduced I_{corr} value from (389 to 64 μA cm^2) and gave inhibition efficiency of 94%. It is also observed that in the presence of polymer both the values of (βa and βc) were increased thereby suggesting that polymer inhibits corrosion by affecting the mechanism of corrosion by participation of polymer in reaction probably in the form of complex $[ms\text{-}BFP]_{ads}$. The dissolution reaction proceeds less readily via adsorbed inhibitor complex than via $[ms\text{-}OH]_{ads}$. Similar observations were reported by Donahue and co-workers [10] that the anodic dissolution of iron is inhibited in presence of aniline derivatives. It is also seen that βc values were more affected than βa values. The E_{corr} value was also shifted in negative direction. Both these observations suggest that polymer predominantly behaves as cathodic inhibitor [11-14].

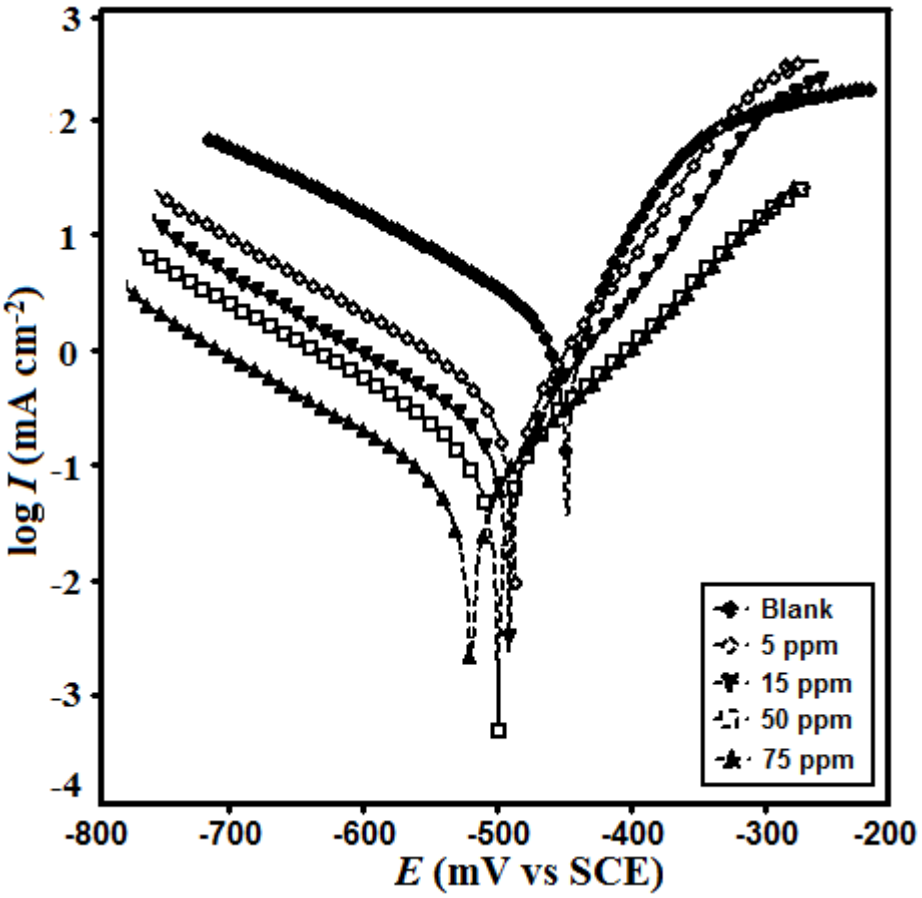

Figure 2. Polarization curves for MS in 1 M HCL and different concentration of BFP polymer.

The linear Tafel area of anodic and cathodic curves was extrapolated to corrosion potential to obtain corrosion current densities (I_{corr}). The inhibition efficiency was evaluated from I_{corr} values using the relationship,

$$\eta\% = \frac{I_{corr} - I_{corr(inh)}}{I_{corr}} \times 100 \quad (3)$$

where I_{corr} and $I_{corr(inh)}$ are the corrosion current density of MS in 1 M HCl in absence and presence of inhibitor.

Polarization resistance (R_p) values were determined from the slope of the potential-current lines. The inhibition efficiency was evaluated from R_p values obtained.

$$\eta\% = \frac{^{inh}R_P - R_P}{^{inh}R_P} \times 100 \quad (4)$$

where $^{inh}R_P$ and R_P was the Polarization resistance of inhibited and uninhibited solution respectively.

3.1.2. Electrochemical impedance spectroscopy (EIS)

The impedance Nyquist Plots ,Bode-phase plots, and equivalent circuit model for mild steel in 1 M HCl in presence and absence of inhibitor are shown in Figure 3 (a-c). The impedance parameters such as charge transfer resistance (R_{ct}), double layer capacitance C_{dl} are given in Table 3. It is seen that the diameter of the semicircles increases with increase in concentrations of BFP, indicating that corrosion is mainly a charge transfer process [15]. The inhibition efficiency is calculated using charge transfer resistance (R_{ct}) as follows,

$$\eta\% = \frac{R_{ct(inh)} - R_{ct}}{R_{ct(inh)}} \times 100 \quad (5)$$

Where $R_{ct(inh)}$ and R_{ct} are the values of charge transfer resistance in presence and absence of inhibitor in 1 M HCl respectively.

Table 3. Electrochemical impedance parameters and corresponding efficiencies for MS in 1 M HCl at different concentration of BFP polymer

Inhibitor concentration(ppm)	R_{ct} (Ω cm^2)	n	Yo ($10^{-6}\Omega^{-1}$ cm^{-2})	C_{dl} (μF cm^{-2})	η%
Blank	12.1	0.868	242.6	100.6	-
5	59.2	0.841	210.0	93.9	79.4
15	75.9	0.818	196.0	81.3	83.9
50	208.1	0.830	130.9	60.0	94.1
75	384.9	0.811	108.1	47.3	96.8

It is also observed from the results that R_{ct} value increases on addition of polymer and highest inhibition efficiency of 96.8% was observed at 75 ppm. The double layer capacitance C_{dl} decreases with increasing concentration of inhibitor due to adsorption of inhibitor molecules on metal surface and increasing thickness of double layer [16-17].

The values of double layer capacitance, C_{dl} was calculated from equation,

$$C_{dl} = Y_0 (\omega_{max})^{n-1} \quad (6)$$

where Y_0 is CPE coefficient, n is CPE exponent (phase shift), ω is the angular frequency.

The thickness of this protective layer (d) is correlated with C_{dl} by the following equation.

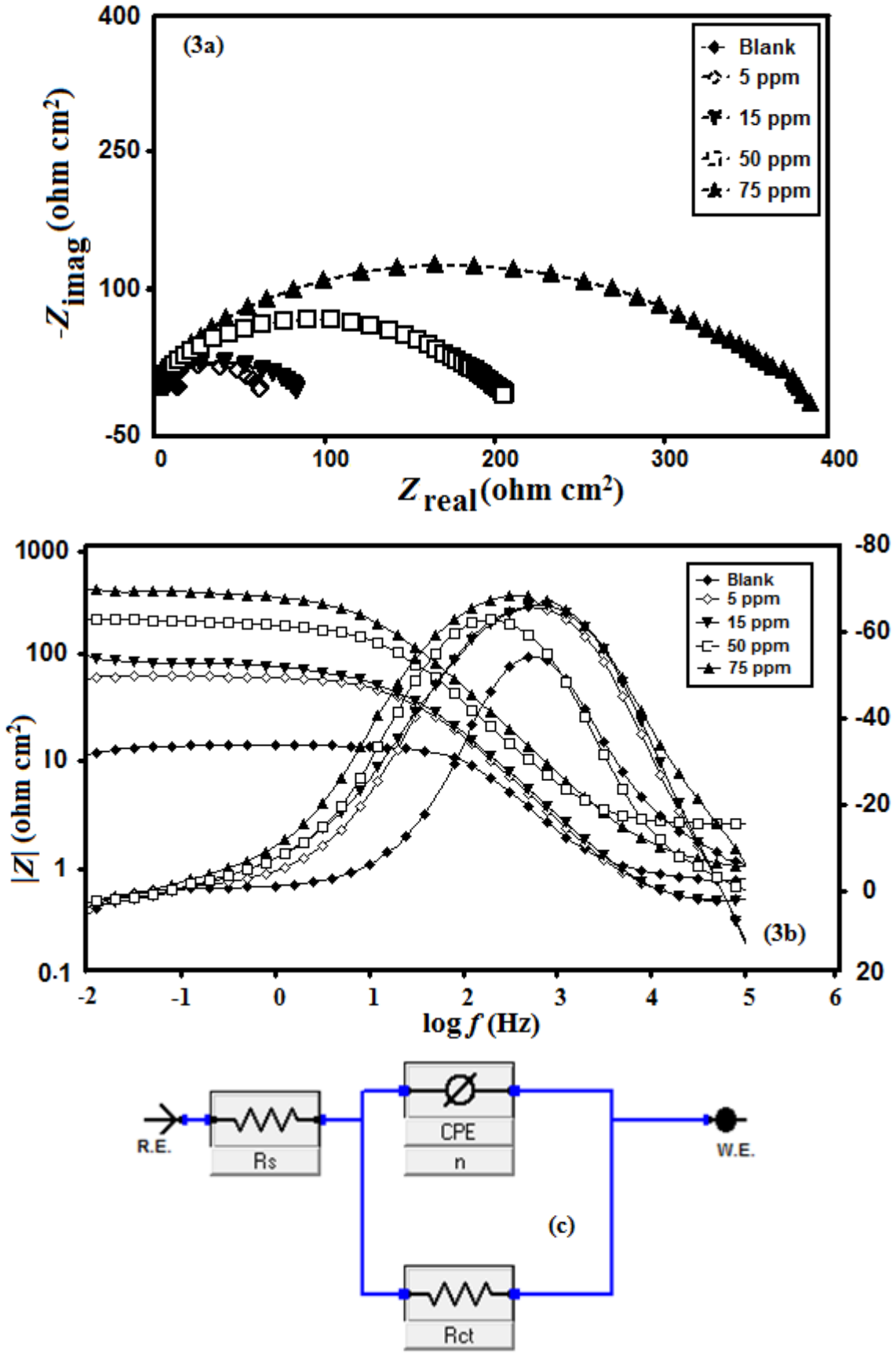

Figure 3. (a) The Nyquist plot (b) Bode-phase angle plot of mild steel in 1 M HCL containing different concentrations of BFP polymer and (c) equivalent circuit model.

$$C_{dl} = \frac{\varepsilon \varepsilon_o A}{d} \quad (7)$$

where ε is the dielectric constant and ε_0 is the permittivity of free space and A is surface area of the electrode.

The obtained values for Bode-phase plots are given in Table 4. The values of phase angle ($-\alpha°$) and slope ($-S$) in polymer are 54.29 and 0.67 respectively. On addition of optimum concentration of polymer the values are ($-\alpha°$) 68.41 and ($-S$) 0.78.The deviation of these values from ideal values ($-\alpha°$) 90 and ($-S$) -1 suggest non ideal behaviour of capacitance. The higher the value of |Z| implies that the polymer inhibits corrosion by forming a protective film on the metal surface.

Table 4. Slopes of the Bode plots at Intermediate Frequencies (S) and the Maximum Phase angles ($\alpha°$) for Mild Steel in 1 M HCl solution with increasing BFP polymer concentrations

Inhibitor concentration(ppm)	$-\alpha°$	$-S$
Blank	54.29	0.67
5	65.71	0.74
15	66.06	0.74
50	62.84	0.73
75	68.41	0.78

3.2. Gravimetric Measurements

3.2.1. Effect of inhibitor concentration

The effect of different concentration of inhibitors was studied by weight loss technique. The results are given in Table 5.It is seen that inhibition efficiency increase with increasing polymer concentrations and best inhibition efficiency obtained 99.0% at 75 ppm concentration.This may be due to the adsorption of polymer molecules leading to the formation of a smooth layer on metal surface which prevents the contact of metal with the surrounding acidic environment and higher bonding ability of inhibitor on the mild steel surface is due to the higher number of lone pairs on heteroatom's and π orbital's[18].

Table 5. Weight loss measurements for MS in 1 M HCl at different concentrations of the BFP polymer

Inhibitor concentration(ppm)	C_R (mm/y)	θ	η (%)
Blank	74.20	-	-
5	8.16	0.89	89.0
15	2.59	0.96	96.5
25	1.85	0.97	97.5
50	1.48	0.98	98.0
75	0.74	0.99	99.0
100	0.74	0.99	99.0

3.2.2. Adsorption isotherm

Adsorption isotherm gives information about the interaction of inhibitor molecules on mild steel surface.The corrosion inhibition mechanism depends on adsorption of inhibitor on metal surface. The adsorption of polymer on metal surface reduces the surface area available for corrosion. [19]. The surface coverage (θ) was calculated according to the following equation,

$$\theta = \frac{C_R - {}^{inh}C_R}{C_R} \quad (8)$$

where, C_R and ${}^{inh}C_R$ is the corrosion rate of MS in absence and presence of inhibitor respectively.

Fitting the degree of surface area coverage value (θ) to adsorption isotherms including Frumkin, Temkin, and Langmuir isotherms, the best fit was obtained in the case of Langmuir adsorption isotherm and according to Langmuir isotherm, surface coverage is related to inhibitor concentration (C_{inh}) by the following equation,

$$\frac{C_{(inh)}}{\theta} = \frac{1}{K_{(ads)}} + C_{(inh)} \quad (9)$$

A straight line was obtained on plotting (C/θ) vs C for Langmuir isotherm with regression coefficient ($R^2 = 1$) confirm this approach as shown in Figure 4.

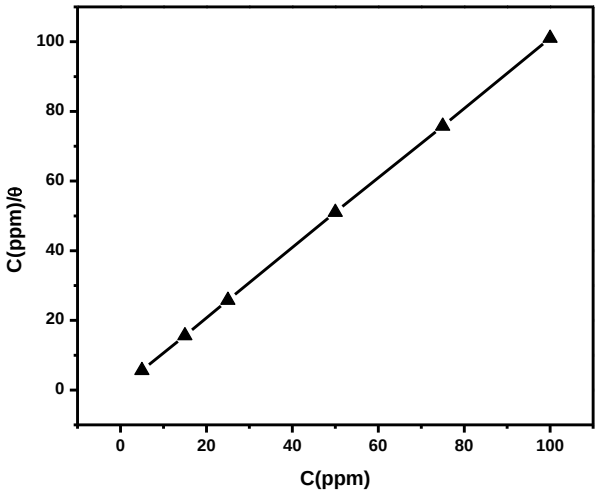

Figure 4. The Langmuir adsorption isotherm plots for MS at different concentrations of BFP polymer with 1M HCl.

3.2.3. Thermodynamic activation parameters

With a view to examine the effect of temperature on corrosion process in presence of polymer the Arrhenius equation was used,

Table 6. Thermodynamic parameters for mild steel in 1 M HCl in absence and presence of BFP *polymer*

Inhibitor concentration(ppm)	*E*a ($kJmol^{-1}$)	ΔH^* ($kJmol^{-1}$)	ΔS^* ($Jmol^{-1}\ K^{-1}$)
Blank	38.15	35.47	-93.62
100	95.16	92.48	54.62

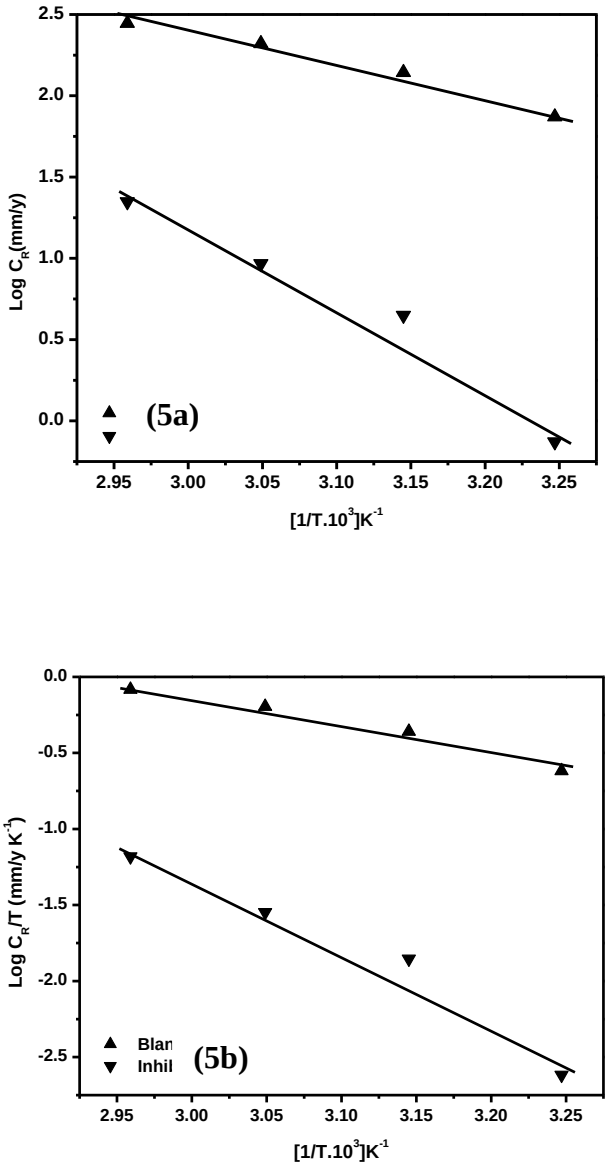

Figure 5. Adsorption isotherm plots (a) log C_R vs. 1000/T (b) log C_R/T vs. 1000/T for MS in 1M HCl in the absence and the presence BFP polymer

$$\ln(C_R) = \frac{-E_a}{RT} + A \qquad [10]$$

where E_a is activation energy, R is the gas constant, A the Arrhenius pre-exponential factor and T is the absolute temperature. A plot of the corrosion rate ln C_R vs 1000/T gives a straight line as shown in Figure 5(a).

From the observed values given in the Table 6 it is observed that the presence of polymer increased activation energy values and consequently decrease in the metal desolation rate. The finding indicate that polymer act as inhibitor and effect on corrosion process through increase the activation energy of metal dissolution by forming a barrier to mass and charge transfer by getting adsorbed on the metal surface[20].

A plot of ln (C_R /T) against 1000/T shown in Figure 5(b) which give straight lines with a slope of (-$\Delta H^*/R$) and an intercept of [(ln(R/Nh)) + ($\Delta S^*/R$)] to which the values of ΔH^* and ΔS^* are calculated and are given in Table 6.

The ΔH^* is the enthalpy of activation and ΔS^* is the entropy of activation can be calculated by given equation,

$$C_R = \frac{RT}{Nh}\exp\left(\frac{\Delta S^*}{R}\right)\exp\left(-\frac{\Delta H^*}{RT}\right) \quad (11)$$

Where h is Plank constant, N is Avogadro's number, ΔS^* is the entropy of activation and ΔH^* is the enthalpy of activation.

The positive signs of enthalpies (ΔH^*) reflect the endothermic nature of dissolution of inhibitor on metal surface. [21]. The shift towards positive value of entropies(ΔS^*) suggested of corrosion that the activated complex in the rate determining step represents dissociation rather than association, meaning that disordering increases on going from reactants to the activated complex[22-23].

3.3. Surface characterization by Optical microscopy

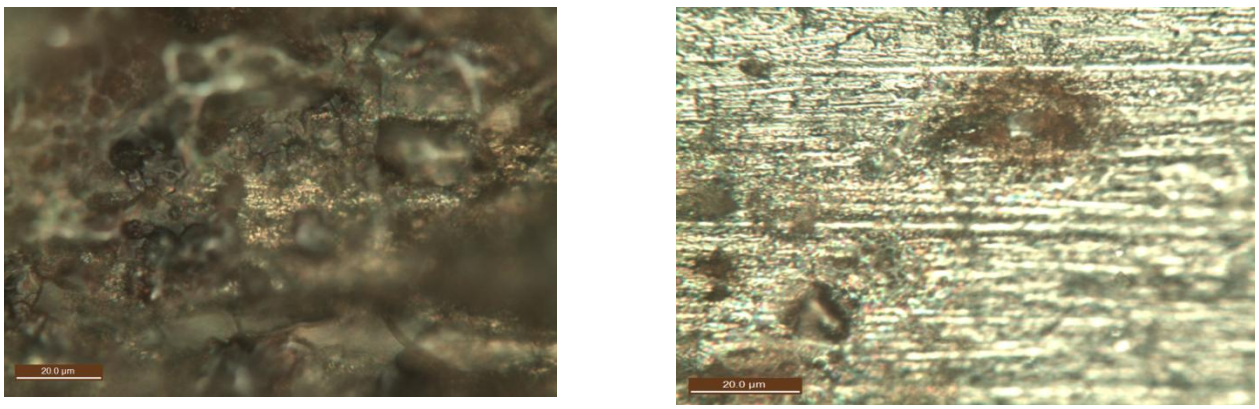

A **B**

Figure 6. Optical microscopy of (a) mild steel in HCl, (b) mild steel in 1 M HCl with BFP polymer

The mild steel surface was examined by Optical microscopy in presence and absence of BFP polymer in 1 M HCl and the results are shown in Figure 6. Figure 6(a) showed the damaging of mild

steel surface because of dissolution of MS due to the surface attack by the aggressive acid solution. In presence of polymer a smooth surface of metal is shown in Figure 6(b). The presence polymer retards metal dissolution because a thin layer of polymer formation takes place on MS surface which forms a barrier between metal and acid solution. [24]

3.4. Mechanism of adsorption and inhibition

The mechanism of corrosion inhibition involves adsorption of polymer on metal surface(Figure 7) in following ways

(i) The electrostatic interaction of protonated BFP with already adsorbed chloride ions on metal surface (physisorption).(ii) donor–acceptor interactions between the π-electrons of aromatic ring and vacant d-orbital of surface iron atoms (reterodonation) and (iii) The donation of unshared pairs of electron of heteroatoms to vacant d-orbital metal[25-26].

$$[\mathrm{BFP}] + x\mathrm{H}^{+} \leftrightarrow [\mathrm{BFP}_{x}]^{x+}$$

The adsorption of inhibitor prevents the electrochemical reaction i.e. the anodic and cathodic reaction on metal surface by forming a a layer of adsorbed inhibitor molecules on metal surface. which protects metal from corrosion [27].

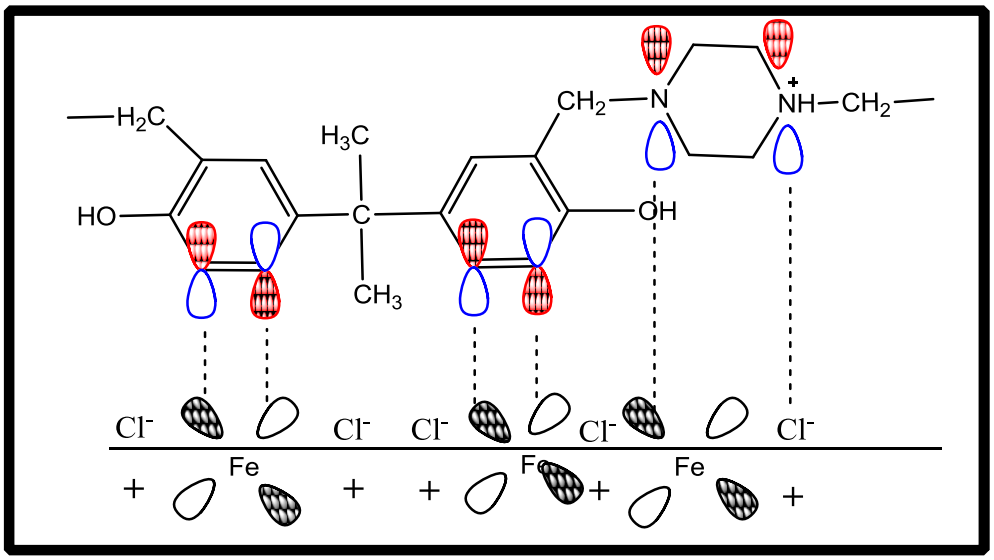

Figure 7. Pictorial representation of mechanism of adsorption of BFP polymer on MS surface

4. CONCLUSIONS

The results of the investigation of polymer (BFP) showed that BFP behaves as a good corrosion inhibitor for MS in 1 M HCl. Polarization data reveals that the inhibitor is mixed-type inhibitor and predoominantly acts as cathodic inhibitor. Polymer increases R_{ct} values and decreases C_{dl} values. The adsorption model obeys Langmuir adsorption isotherm.

ACKNOWLEDGEMENTS
Priyanka Singh is thankful to UGC New Delhi for the Project (40-101/2011) SR, Fellowship.

References

1. S.Y. Lin, Y. Isome, E. Stewart, J.F. Liu, D. Yohannes, L. Yu, *Tetrahedron Lett.* 47 (2006) 2883
2. T. Grchev, M. Cvetkovska, J.W. Schultze, *Corros. Sci.* 32 (1991) 103
3. P. Manivel, G. Venkatachari, *J. Appl. Polym. Sci.* 104 (2007) 2595
4. P. Manivel, G. Venkatachari, *J. Met. Mater. Sci.* 46 (2004) 165
5. M. Schorr, J. Yahalom, *Corros. Sci.* 12 (1972) 867
6. Practicals in Polymer Science, 1st ed., Siddaraman, CBS Publishers Bangalore (2005) 43
7. S. Sathiyanarayanan, S.K. Dhawan, D.C. Trivedi, K. Balakrishnan, *Corros. Sci.* 33 (1992) 1831
8. P. Manivel, G. Venkatachari, *J. Mater. Sci. Technol*. 22 (2006) 301
9. N. Nishat, T. Ahamad, S. Ahmad, S. Parveen, *J. Coord. Chem*. 64 (2011) 2639
10. F. M. Donahue, K. Nobe, *J.electrochem. Soc.* 114 (1967)1012
11. M. Gopiraman, N. Selvakumaran, D. Kesavan, I. S. Kim, R. Karvembu , *Ind. Eng. Chem. Res*. 51 (2012) 7910
12. I. Ahamad, R. Prasad, M.A. Quraishi, *Corros. Sci*. 52 (2010)1472
13. S.M.A. Hosseini, A. Azimi, *Corros. Sci*. 51 (2009) 728
14. M. Ajmal, A.S. Mideen, M.A. Quraishi, *Corros. Sci.* 36 (1994) 79
15. S. Zhang, Z. Tao, W. Li, B. Hou, *Appl. Surf. Sci.* 255 (2009) 6757
16. H. Ashassi-Sorkhabia, B. Shaabanib, D. Seifzadeha, *Electrochim. Acta* 50 (2005) 3446
17. Z. Tao, S. Zhang, W. Li, B. Hou, *Corros. Sci.* 51 (2009) 2588
18. H. Ashassi-Sorkhabi, D. Seifzadeh, M.G. Hosseini, *Corros. Sci*. 50 (2008) 3363
19. M. Gopiraman, N. Selvakumaran, D. Kesavan, R. Karvembu, *Prog. Org. Coat*. 73 (2012)104
20. A. Singh, I. Ahamad, V. K. Singh, M. A. Quraishi, *J Solid State Electr*. 15 (2011) 1087
21. I. Ahamad, M.A. Quraishi, *Corros. Sci*. 52 (2010) 651
22. D. K. Yadav, B. Maiti, M.A. Quraishi, *Corros. Sci*. 52 (2010) 3586
23. G. ji, S. K. Shukla, P. Dwivedi, S. Sundaram, R. Prakash, *Ind. Eng. Chem. Res*. 50 (2011)11954
24. Dae-K. Kim, S. Muralidharan, Tae-H. Ha, Jeong-H. Bae, Yoon-C. Ha, Hyun-G. Lee, J.D. Scantlebury, *Electrochim. Acta* 51 (2006) 5259
25. D. K. Yadav, M. A. Quraishi, *Ind. Eng. Chem. Res*. 51 (2012) 8194
26. I. Ahamad, R. Prasad, M.A. Quraishi, *Mater. Chem. Phys*. 124 (2010) 1155
27. M.A. Quraishi, A. Singh, V. K. Singh, D. K. Yadav, A. K. Singh, *Mater.Chem. Phys*. 122 (2010)114

© 2013 by ESG (www.electrochemsci.org)